3876 *Macromolecules* **2010**, *43*, 3876–3881
DOI: 10.1021/ma100168g

Macromolecules
ARTICLE

Phase Behavior and Proton Conduction in Poly(vinylphosphonic acid)/Poly(ethylene oxide) Blends

Fengjing Jiang,[†,‡] Haijin Zhu,[†] Robert Graf,[†] Wolfgang H. Meyer,*[,†] Hans W. Spiess,[†] and Gerhard Wegner[†]

[†]*Max Planck Institute for Polymer Research, Ackermannweg 10, Mainz 55128, Germany, and* [‡]*Shanghai Jiao Tong University, 800 Dongchuan Rd., Shanghai 200240, China*

Received January 22, 2010; Revised Manuscript Received March 2, 2010

ABSTRACT: The miscibility of poly(vinylphosphonic acid) (PVPA) and poly(ethylene oxide) (PEO) is studied for the first time in this work, and a miscibility diagram is obtained based on thermoanalytical (DSC) and optical microscopy data. On the basis of this knowledge, homogeneous PVPA/PEO blends are prepared as proton-conducting polymer films. The mobility of phosphonic acid groups and PEO in the blends is determined by ^{1}H-MAS NMR in temperature-dependent measurements. The effect of composition and the role of PEO on proton conduction are discussed.

Introduction

Proton conduction in solid-state polyelectrolytes has aroused considerable interest in recent years since new materials for fuel cells are investigated.[1−8]

In water-free proton-conducting solid polyelectrolytes, proton transfer can be carried out only by hydrogen bond breaking and forming processes because there is no mobile species other than protons. In poly(vinylphosphonic acid) (PVPA), proton migration via a Grotthuss type mechanism contains two steps: (1) displacement of a proton along a hydrogen bond; (2) transfer of the proton to another "proton solvent" (oxygen) with formation of a new hydrogen bond.[5,9] The rearrangement of hydrogen bonds is supported by a high local mobility and "free volume", and the total mechanism can be described as "structure diffusion" because the proton transport is depending on the motion of a structural defect of the hydrogen bond system.[10]

PVPA was considered to be one of the most promising anhydrous proton conductors due to the very high density of phosphonic acid moieties. However, the proton conductivity of PVPA was not as high as expected, and the activation energy was around 60 kJ/mol.[11] Compared with liquid phosphonic acid which exhibits a very high proton conductivity and low activation energy, the discrepancy is large and is probably caused by the limitation of molecular motion.[12,13]

PEO has a much lower glass transition temperature (210 K) than PVPA and contains abundant oxygen atoms in the backbone chain which can form hydrogen bonds with phosphonic acid groups. These characteristic properties were considered to be helpful to build a dynamic hydrogen bond network in PVPA/PEO blends. Indeed, proton transport between hydrogen-bonded sites by PEO has been shown in imidazole-based proton conductors.[14,15]

Miscibility of polymers is of great importance for properties such as thermal stability, mechanical rigidity, dielectric loss, and optical transparency. The phase diagram of PVPA and PEO, however, has not been studied to the best of our knowledge. Therefore, the miscibility of PVPA/PEO blends and the effect of blending on proton conductivity are considered here for the first time.

*Corresponding author: Fax +49 6131 379-480; e-mail meyer@mpip-mainz.mpg.de.

Experimental Section

Materials. PVPA was synthesized with anionic polymerization. The details of the anionic synthesis of homo- and block copolymers of PVPA will be reported in a separate publication.[16] PEO (M_w = 20 000, Aldrich) was used as received.

Preparation of PVPA/PEO Blends. PVPA and PEO were first dissolved in deionized water to obtain a homogeneous solution. Second, the solution was cast onto glass substrates. Then, the glass substrates were flushed with dry nitrogen for 1 week and dried under vacuum (10^{-3} Pa) for 48 h in order to remove the solvent.

^{1}H MAS NMR experiments were carried out with a 850 MHz (Bruker Avance II 850 spectrometer), with a spinning frequency of 25 kHz and 30 kHz, respectively.

Thermal Gravimetric Analysis (TGA). TGA was performed on a TGA/SDTA851 (Mettler Toledo) under N_2 with a heating rate of 10 K/min.

Differential Scanning Calorimetric (DSC). PVPA/PEO mixtures have been prepared by using water as the common solvent of PVPA and PEO. The samples for DSC measurements were freeze-dried. During the DSC measurements, the samples were first heated to 150 °C (first scan) and then quenched to −100 °C (second scan) followed by the third scan (heating to 150 °C again). DSC was performed on a DSC 822 (Mettler Toledo) under N_2 with a heating rate of 10 K/min.

Optical Microscopy. Optical microscopy images were recorded on a Zeiss Axiophot microscope equipped with a CCD camera (AxioCam). All samples were measured on a heating plate protected with a nitrogen atmosphere. The heating rate was 10 K/min. Diluted solutions of PVPA and PEO in water were used for film casting. Afterward, the glass substrates were flushed with dry nitrogen for 1 week and then dried under vacuum (10^{-3} Pa) for 48 h in order to remove the solvent completely.

Proton Conductivity. Proton conductivity was measured by dielectric spectroscopy in a two-electrode geometry using an SI 1260 impedance/gain-phase analyzer in the frequency range of 10^{-1}−10^{-6} Hz. All samples were dried at 50 °C under vacuum (10^{-3} Pa) for 4 days prior to the measurements. Dry N_2 was used

 Published on Web 03/08/2010

to flush the samples during the measurements. The samples for conductivity measurements were pressed to tablets and contacted by E-tek and stainless steel electrodes.

Wide-Angle X-ray Scattering (WAXS) was performed to investigate the structure of the PVPA/PEO blends in the process of cooling from 90 to −50 °C.

Results and Discussion

Thermal Analysis of PVPA/PEO Blends. In the following discussion, the abbreviation PVPE refers to PVPA/PEO polymer blends. For example, PVPE (10%) means that the PVPA/PEO blend contains 10% PEO by weight ratio. Figure 1 shows the results of TGA measurements of pure PEO and PVPEs with various compositions. In the TGA curves, two degradation steps can be identified. The first step refers to the degradation of PEO since it scales with the PEO content. The second step indicated the degradation of PVPA and may to a large extent be caused from water loss and anhydride formation, since a considerable residue remains even at temperatures above 500 °C. PEO itself is stable until about 400 °C, and its degradation temperature decreases dramatically upon blending with PVPA. This shows that PEO is less thermally stable in an acidic environment and indicates a close interaction between PVPA and PEO.

The DSC results are shown in Figure 2. There is no melting transition which can be attributed to the melting of ice in all DSC curves. Therefore, it can be considered that no freezable water is contained in the samples.

PVPEs with low PEO content show no peak in the first scan (see Figure 2a). In the second scan, two exothermic peaks (peaks i and ii) appear between −50 and −10 °C. Peak iv in the third scan is the melting peak of crystalline PEO. The total integration of peaks i and ii is close to that of peak iv, which indicates that crystalline PEO is formed during the cooling procedure and both peaks i and ii are recrystallization peaks of PEO. However, the reason for the different crystallization temperatures (peaks i and ii) is not clear yet.

In Figure 2b, the endothermic peak in the first scan around 60 °C (peak iii) is the melting peak of the PEO crystals which originally exist in the blends. In the second scan three crystallization peaks are observed. The total integration of the exothermic peaks (i + ii + v) is close to that of peak iv, which means that peak iv is the melting peak of the total PEO crystals formed in peaks i, ii, and v, respectively.

PVPE with Low PEO Contents. On the basis of the above discussion, it can be concluded that, at low PEO contents (< 50 wt %): (1) PVPA and PEO are miscible, and homogeneous PVPA/PEO blends can be obtained. (2) The blends are metastable, and phase separation can occur at T_c, the critical temperature of phase separation, which leads to small PEO droplets dispersed in the PVPA matrix. At $T > T_m$, the PEO droplets are amorphous. (3) The chain mobility of PEO within these droplets may be restricted by the interaction with PVPA chains, since it must be assumed that the droplets contain a mixed rather than a pure PEO phase. Moreover, there should also be hydrogen bonding on the interlayer between the PEO droplet phase and the PVPA matrix phase. These two factors may explain the two crystalline peaks (peaks i and ii) at low temperatures. When being quenched to −50 °C, pure PEO crystallizes in the PEO droplets. (4) When heated again to $T > T_m$, the PEO crystals melt. (5) The phase separation is irreversible. These processes are schematically shown in Scheme 1.

PVPA with High PEO Contents (*> 50 wt %*). (1) PVPA and PEO are only partially miscible. Therefore, a homogeneous PVPA/PEO mixed phase and a PEO-rich phase with crystalline PEO coexist. (2) The PVPA/PEO blend is metastable, and further phase separation occurs at $T_c > T_m$, leading to small amorphous PEO droplets dispersed in the PVPA matrix while the residual PEO phase becoming amorphous. (3) Upon cooling, the PEO in the small droplets crystallizes in the temperature range between −50 and −10 °C (peaks i and ii), while PEO in the original pure PEO phase crystallizes at round 40 °C (large droplets, peak v). (4) Being heated to $T = T_m$, the PEO melts. Both small and large droplets coexist in the blends. (5) The phase

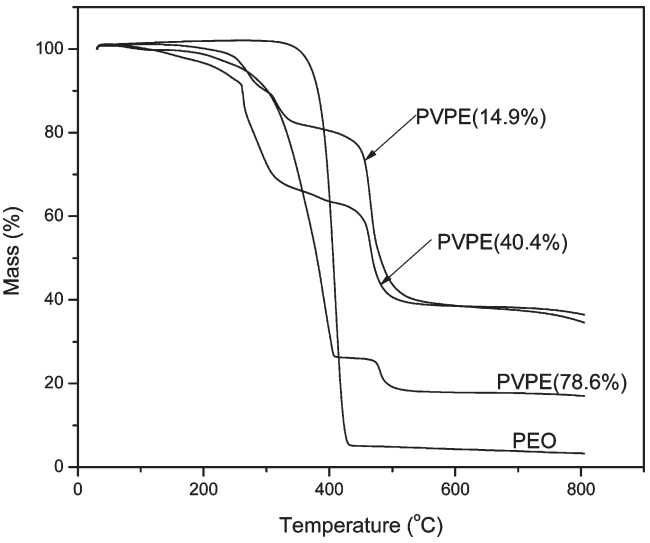

Figure 1. TGA curves of PEO and PVPA/PEO blends measured under dry nitrogen.

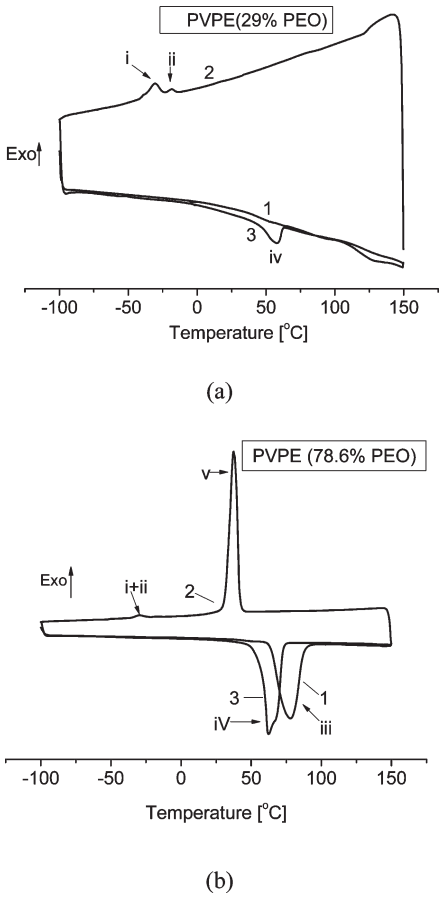

Figure 2. DSC curves of PVPE with various PEO content.

separation is irreversible. These processes are schematically shown in Scheme 2.

Miscibility Diagram of PVPA/PEO Blends. *Phase Separation Observed by Optical Microscopy*. For optical microscopy film samples were used. Figure 3 shows the image of a PVPE (31%) observed in the polarized mode. At 20 °C, the membrane is homogeneous and transparent (Figure 3a). After being heated to 140 °C, heterogeneities develop (Figure 3b). A similar phenomenon can be observed in the blends with various PEO contents less than 50 wt %, but phase separation occurs at different temperatures. When the PEO content exceeds 50%, PEO crystals can be observed already at 20 °C without any annealing history, and the heterogeneity of the membrane remains even at 150 °C. Therefore, phase separation (if there is) cannot be observed by optical microscopy in the PVPA/PEO mixture with more than 50 wt % PEO.

Phase Separation Observed by DSC. As discussed above, the blends of PVPA and PEO are metastable to a large extent. Thus, phase separation can be induced at high temperatures. As a result, a crystallization peak of PEO in the droplets can be detected below −10 °C.

Scheme 1. Schematic Illustration of the Phase Behavior of PVPE with Low PEO Contents

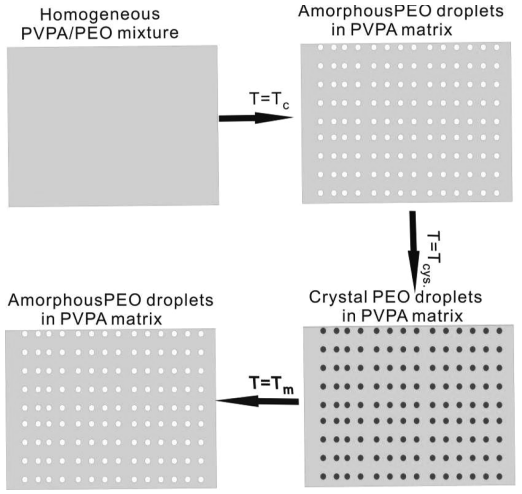

For further investigations the following temperature program was used for the DSC measurements: (1) increasing the temperature from −50 °C to a temperature T_1 and then cooling down again to −50 °C with 10 K/min (T_1 cycle); (2) increasing the temperature to T_2, which is a little higher than T_1 (T_2 cycle, 10 K/min); (3) continue with other temperatures cycles until the crystallization peak appears in the cooling procedure.

The temperature cycle in which the crystallization peak appears first is the temperature at which phase separation starts (T_c). When the sample is heated to $T > T_c$, the intensities of the crystallization peaks increase with increasing T (see Figure 4) because phase separation is a relaxation phenomenon and its extent increases with time and temperature.

On the basis of the determination of T_c via optical microscopy and DSC, the miscibility diagram of PVPA/PEO blends is plotted in Figure 5. The region below the separation temperatures is the one-phase region in which PVPA and PEO are miscible and homogeneous films can be obtained. The region above the separation temperatures is the two-phase region in which PVPA and PEO are only partly miscible. The boundary with hollow symbol was obtained with optical microscopy, and the boundary of solid symbol was derived from the DSC results. The discrepancy of the two boundaries may result from the different time and geometrical scale at which phase separation was detected in the optical microscope as compared to DSC. Phase separation observed with optical microscopy is of micrometer scale. With the same heating rate, the temperature for phase separation at that scale is much higher than that at nanoscale as in DSC since the heat flux to the larger particles happens on a slower time scale than that to nanoparticles.

Proton Magic-Angle-Spinning NMR. Nuclear magnetic resonance (NMR) spectroscopy is a powerful tool to determine local structural arrangements as well as their dynamics. Particularly, high-resolution ultrafast ^{1}H MAS NMR provides specific information on hydrogen bonding and chain motion.

Proton mobility is a precondition for proton conduction. In fully solid-state polyelectrolytes, proton motion is often connected with various types of chain motions. Therefore, the detection of local chain dynamics is of great importance to understand the proton transport mechanism.

Scheme 2. Schematic Illustration of the Phase Behavior of PVPE with High PEO Content (> 50 wt %)

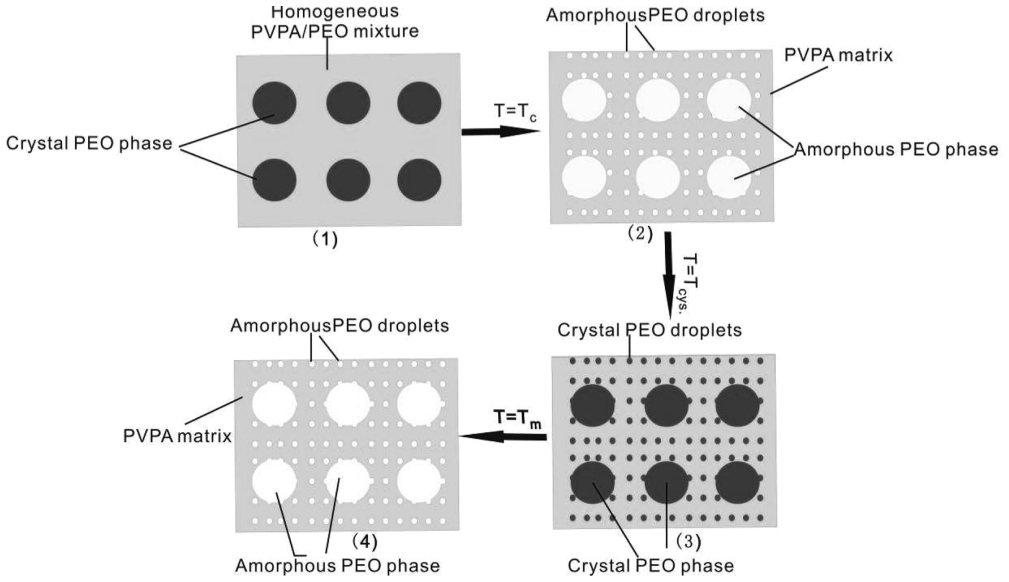

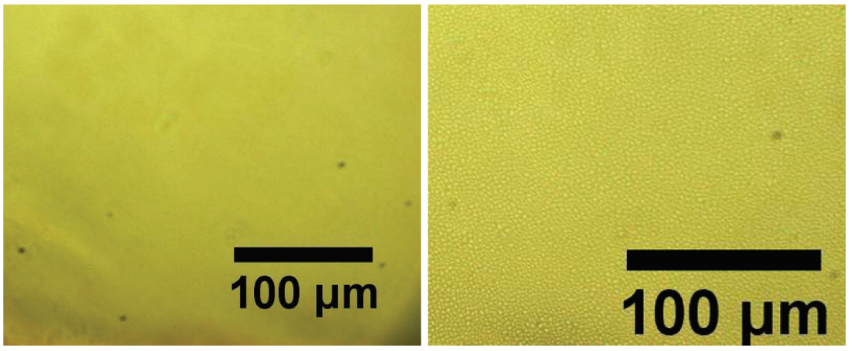

Figure 3. Polarized optical images of PVPE (31%) at (a) 20 °C and (b) 140 °C.

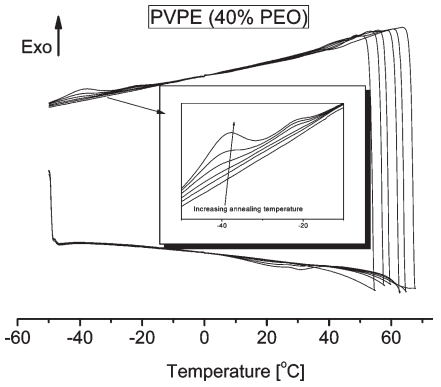

Figure 4. DSC curves of PVPE (40%) measured in increasing temperature cycles.

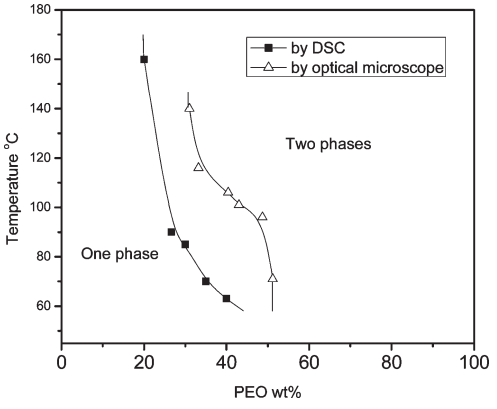

Figure 5. Miscibility diagram of PVPA/PEO blends.

An 850 MHz NMR spectrometer was applied to study the local dynamics of the PVPA/PEO blends. ^{1}H MAS NMR spectra of PVPA, PEO, and their blends with various compositions are shown in Figure 6. The peak at 10.6 ppm is the resonance peak of the proton at the POH groups. The peak at around 3.8 ppm derives from CH_2 of PEO. The broad peak at 2.2 ppm refers to CH_2 and CH from the PVPA backbones. We can see that the CH_2 peak from PEO is very sharp, which indicates fast chain motion of the PEO backbone chains. However, the resonance peak from the PVPA backbone chain is broad as compared with PEO which shows poor mobility of the PVPA chains.

In the ^{1}H MAS NMR spectra of PVPA, the peak of the POH narrows with increasing temperature which indicates improved proton mobility at high temperatures. However,

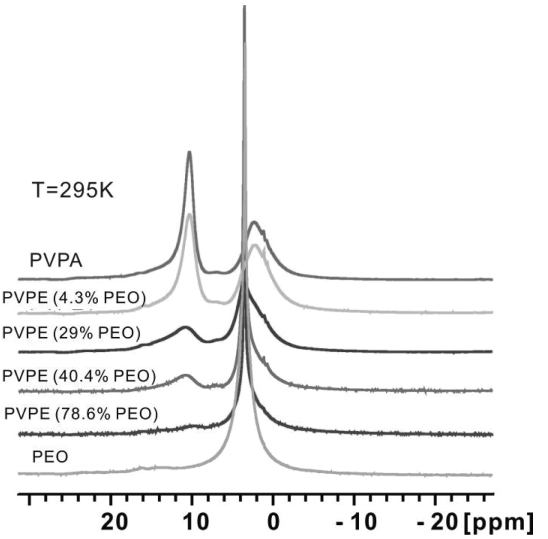

Figure 6. ^{1}H MAS NMR spectra of PVPEs at 25 °C.[17]

the peak from the PVPA backbone chain does not change with temperature because PVPA is still in the glassy state and the motion of the PVPA backbone remains very limited even at 393 K.[10]

^{1}H MAS NMR spectra of PVPE (4.3%) measured with increasing temperature are shown in Figure 7. At 295 K, the CH_2 peak from PEO is embedded in the broad peak of the PVPA main chains. Because of the full miscibility at 4.3% PEO content, the PEO chains can be assumed to interact with the PVPA chains and multiple hydrogen-bonding between PVPA and PEO chains is highly probable. Therefore, the mobility of the PEO chains is restricted, which leads to a broad peak which overlaps with that of PVPA. At elevated temperatures, the mobility of the PEO increases; the peak narrows, while the peak of the PVPA backbone remains broad. After heating, the sample was cooled down to 300 K again, and the peak of PEO broadens and finally disappears again. This means that the described phenomenon is reversible in PVPE (4.3%) (see Figure 8).

With PVPE (29%), the mobility of the PEO also increases with temperature. Upon cooling, however, the peaks of the PEO chains remain sharp. Figure 9 shows the ^{1}H MAS NMR spectra of PVPE (29%) before and after annealing. After annealing at 120 °C, the peak of the PEO is much sharper than before annealing, which means that the mobility of the PEO chain is irreversibly improved. According to the miscibility diagram in Figure 5, irreversible phase separation in PVPE (29%) already happens at 120 °C. Both results

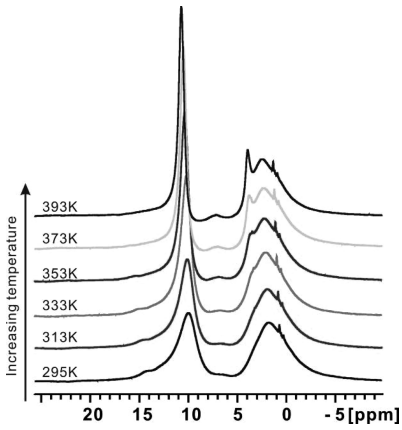

Figure 7. ^{1}H MAS NMR spectra of PVPE (4.3%) measured with increasing temperature.[17]

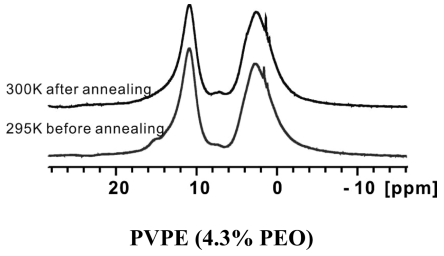

Figure 8. ^{1}H MAS NMR spectra of PVPE (4.3%) before and after annealing.[17]

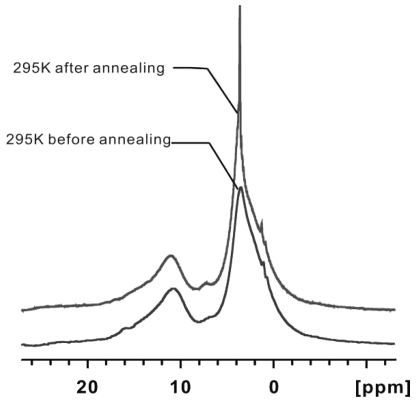

Figure 9. ^{1}H MAS NMR spectra of PVPE (29%) before and after annealing.[17]

may be interpreted such that increased phase separation upon annealing leads to improved PEO chain mobility, but not an increased mobility of the PVPA chains.

Proton Conduction of PVPA/PEO Blends. Anhydrous proton conductivities of PVPA/PEO blends measured in heating−cooling cycles are shown in Figure 10. The proton conductivity decreases with increasing PEO content in the mixture. The lower conductivity in the cooling cycle may be due to the self-condensation of the phosphonic acid groups. All of the conductivities show Arrhenius type of behavior. For each sample, the activation energies in both heating and cooling cycle are exactly the same, which means in these cases self-condensation only changes the number of "mobile protons" but not the mobility. Here the term "mobile protons" refers to the protons that can contribute to conductivity.

The proton conduction activation energies were calculated from the Arrhenius plots in Figure 10 and shown in

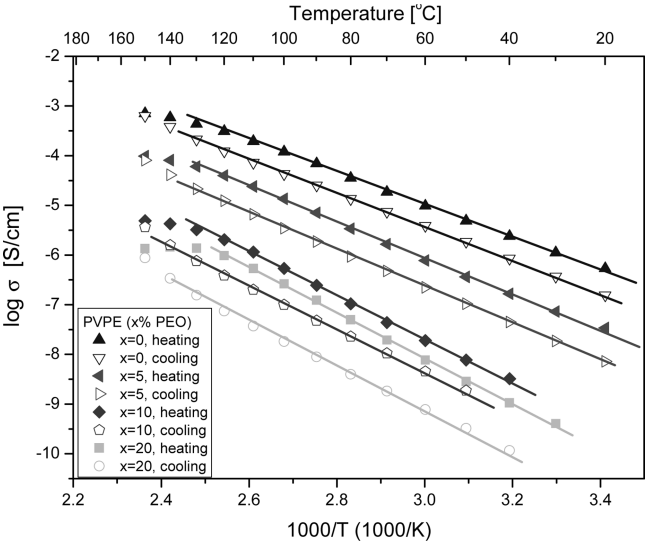

Figure 10. Arrhenius plots of proton conductivities of PVPA/PEO blends measured in dry conditions (solid: heating; hollow: cooling).

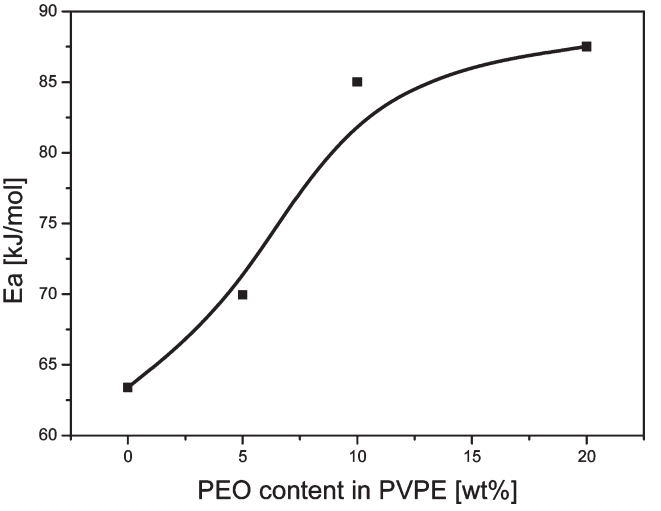

Figure 11. Activation energy of proton conduction in PVPEs with various PEO contents.

Figure 11. The activation energy increases with increasing PEO content. This maybe interpreted such that the pathway for long distance proton transport becomes increasingly limited with increasing PEO content.

From Figure 10 it becomes clear that the proton conductivity of PVPE shows Arrhenius type behavior, which means that the polymer chain motion has no notable effect on proton conductivity. Figure 12 shows the Arrhenius plot of proton conductivities of PVPE (30%) measured in a heating−cooling cycle. In the heating cycle, below 80 °C, proton conductivity still shows an Arrhenius type behavior; however, above 80 °C, the conductivity deviates from the linear part and increases more pronouncedly with increasing temperature. According to the miscibility diagram of PVPE shown in Figure 5, the phase separation temperature (T_c) of PVPE (30%) occurs at 80 °C. Below T_c, the blend is homogeneous and shows Arrhenius type behavior, but when phase separation happens, the PEO content in the PVPA/PEO homogeneous matrix decreases with the consequence that the proton conductivity increases in the leftover matrix phase. After phase separation, the log σ plot of the cooling cycle becomes linear again. However, apparently the

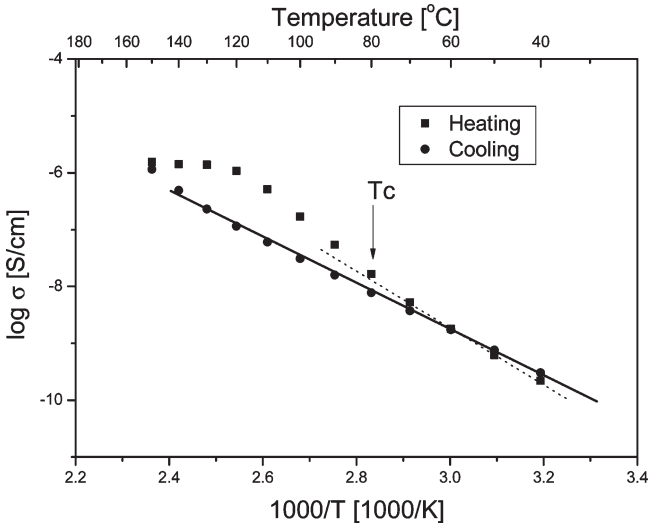

Figure 12. Arrhenius plot of proton conductivities of PVPE (30%).

activation energy decreases from 95 to 78 kJ/mol because the PEO content in the remaining PVPA/PEO matrix phase decreases as a result of the phase separation.

The reason why the activation energy of the proton conduction increases with increasing PEO content yet is not fully understood. Some possibilities are discussed as follows: (1) Proton transport in PVPA can be supported by both rotation of acid groups and motion of the protons. However, the proton motion can be hindered by the PEO chains where the PEO chains maybe considered as proton traps which are deeper than those in pure PVPA, so that the energy to activate the proton motion is higher. (2) The average distance between phosphonic acid groups increases with increasing PEO content. As a result, the connectivity of the phosphonic acid groups is reduced which leads to increasing activation energy with increasing PEO content.

Conclusion

A miscibility diagram of PVPA and PEO has been obtained based on a DSC sand optical microscopy data. Homogeneous PVPA/PEO blends can be prepared as proton-conducting polymer blends. Although the fast mobility of PEO chains was proven by ^{1}H-MAS NMR, the proton conductivity in the blends decreases with increasing PEO content. The PEO chains seem to block the proton transport between the phosphonic acid groups, and this effect leads to increasing apparent activation energies for proton conductivity with increasing PEO content in the blends.

Acknowledgment. The authors thank Angelika Manhart for the synthesis of PVPA and Christoph Sieber for the conductivity measurements. F. Jiang appreciates the scholarship from MPIP. BMBF (project DryD under Contract 03SF0309A) is acknowledged.

Supporting Information Available: A table containing the integrations of the peaks appearing in Figure 2a,b and wide-angle X-ray scattering of the PVPE structure at various temperatures and polarized optical images of PVPE (78.6%) and ^{1}H MAS NMR spectra of PVPA measured with increasing temperature and the Bode plots of ac conductivities of PVPA and PVPEs. This material is available free of charge via the Internet at http://pubs.acs.org.

Note Added after ASAP Publication. This article posted ASAP on March 8, 2010. Several text revisions were made after publication, including the addition of reference 17. The correct version posted on March 12, 2010.

References and Notes

(1) Herz, H. G.; Kreuer, K. D.; Maier, J.; Scharfenberger, G.; Schuster, M. F. H.; Meyer, W. H. *Electrochim. Acta* **2003**, *48*, 2165–2171.
(2) Benhabbour, S. R.; Chapman, R. P.; Scharfenberger, G.; Meyer, W. H.; Goward, G. R. *Chem. Mater.* **2005**, *17*, 1605–1612.
(3) Bozkurt, A.; Meyer, W. H.; Gutmann, J.; Wegner, G. *Solid State Ionics* **2003**, *164*, 169–176.
(4) Celik, S. U.; Akbey, U.; Graf, R.; Bozkurt, A.; Spiess, H. W. *Phys. Chem. Chem. Phys.* **2008**, *10*, 6058–6066.
(5) Lee, Y. J.; Murakhtina, T.; Sebastiani, D.; Spiess, H. W. *J. Am. Chem. Soc.* **2007**, *129*, 12406–12407.
(6) Jiang, F.; Pu, H.; Meyer., W. H.; Guan, Y.; Wan, D. *Electrochim. Acta* **2008**, *53*, 4495–4499.
(7) Jiang, F.; Kaltbeitzel, A.; Fassbender, B.; Brunklaus, G.; Meyer, H. W.; Spiess, W. H.; Wegner, G. *Macromol. Chem. Phys.* **2008**, *209*, 2494–2503.
(8) Britz, J.; Meyer, H. W.; Wegner, G. *Adv. Mater.* **2009**, *21*, DOI: 10.1002/adma.200902834.
(9) Jiang, F.; Kaltbeitzel, A.; Meyer, W. H.; Pu, H.; Wegner, G. *Macromolecules* **2008**, *41*, 3081–3085.
(10) Schuster, M. F. H.; Meyer, W. H. *Annu. Rev. Mater. Res.* **2003**, *33*, 233–261.
(11) Bingoel, B. Synthesis and Characterization of Poly(vinylphosphonic acid) for Proton Exchange Membranes in Fuel Cells. Ph.D. Dissertation, Johannes Gutenberg University, Mainz, 2007.
(12) Bingöl, B.; Meyer, W. H.; Wagner, M.; Wegner, G. *Macromol. Rapid Commun.* **2006**, *27*, 1719–1724.
(13) Lee, Y. J.; Bingöl, B.; Murakhtina, T.; Sebastiani, D.; Meyer, W. H.; Wegner, G.; Spiess, H. W. *J. Phys. Chem. B* **2007**, *111*, 9711–9721.
(14) Schuster, M. F. H.; Meyer, W. H.; Wegner, G.; Herz, H. G.; Ise, M.; Kreuer, K. D.; Maier, J. *Solid State Ionics* **2001**, *145*, 85–92.
(15) Goward, G. R.; Schuster, M. F. H.; Sebastiani, D.; Schnell, I.; Spiess, H. W. *J. Phys. Chem. B* **2002**, *106*, 9322–9334.
(16) Wagner, T.; Manhart, A.; Deniz, N.; Kaltbeitzel, A.; Wagner, M.; Brunklaus, G.; Meyer, W. H. *Macromol. Chem. Phys.* **2009**, *210*, 1903–1914.
(17) The sharp and temperature independent NMR signals around 1 ppm probably originate from the anionic initiator of the PVPA synthesis.